Platinum Monolayer on Nonnoble Metal−Noble Metal Core−Shell Nanoparticle Electrocatalysts for O₂ Reduction

J. Zhang, F. H. B. Lima,[†] M. H. Shao, K. Sasaki, J. X. Wang, J. Hanson, and R. R. Adzic*

Department of Chemistry, Brookhaven National Laboratory, Upton, New York 11973

Received: October 3, 2005; In Final Form: October 28, 2005

We synthesized a new class of O₂ electrocatalysts with a high activity and very low noble metal content. They consist of Pt monolayers deposited on the surfaces of carbon-supported nonnoble metal−noble metal core−shell nanoparticles. These core−shell nanoparticles were formed by segregating the atoms of the noble metal on to the nanoparticles' surfaces at elevated temperatures. A Pt monolayer was deposited by galvanic displacement of a Cu monolayer deposited at underpotentials. The mass activity of all the three Pt monolayer electrocatalysts investigated, viz., Pt/Au/Ni, Pt/Pd/Co, and Pt/Pt/Co, is more than order of magnitude higher than that of a state-of-the-art commercial Pt/C electrocatalyst. Geometric effects in the Pt monolayer and the effects of PtOH coverage, revealed by electrochemical data, X-ray diffraction, and X-ray absorption spectroscopy data, appear to be the source of the enhanced catalytic activity. Our results demonstrated that high-activity electrocatalysts can be devised that contain only a fractional amount of Pt and a very small amount of another noble metal.

Introduction

Considerable attention has been focused on the electrocatalytic oxygen reduction reaction (ORR) because of its slow kinetics and the need for better electrocatalysts with minimal Pt content for fuel-cell cathodes.[1,2−5] A particularly difficult problem is the large loss in potential of 0.3−0.4 V in the initial part of the polarization curves that is the source of a major decline in the fuel-cell's efficiency. This loss was partly attributed to the inhibition of O₂ reduction caused by OH adsorption on Pt in the potential region 0.75−1 V.[2,5,6] Another drawback with existing electrocatalyst technology is the high Pt loading in fuel-cell cathodes.

Several approaches that were explored to ameliorate this disadvantage had limited success, including increased dispersion and alloying Pt with nonnoble transition metals.[6] However, one promising way to solve these problems involves using electrocatalysts made with a Pt monolayer supported on suitable metal nanoparticles.[7,8] In this contribution, we report our development of a new class of the ORR electrocatalysts based on such supported Pt monolayers. Platinum is deposited in a monolayer amount on the surfaces of carbon-supported nonnoble metal−noble metal core−shell nanoparticles. Using the nonnoble metals for cores facilitates a further reduction of the content of the noble metal in the ORR electrocatalysts. In addition, by properly selecting the noble metal shell, the activity of a Pt monolayer can be heightened through electronic and/or geometric effects. The metals constituting the shell and core are chosen considering the segregation properties of the two metals and their electronic and strain-inducing effects on a Pt monolayer. The nonnoble

metal−noble metal core−shell nanoparticles were synthesized by segregating the atoms of the noble metal to the nanoparticle surface at elevated temperatures. A Pt monolayer was deposited on carbon-supported core−shell metal nanoparticles by the galvanic displacement by Pt of a Cu monolayer obtained by underpotential deposition (UPD).[9]

Experimental Section

The synthesis of core−shell nanoparticles involved first impregnating the Vulcan X-72C carbon with mixed solutions of noble and nonnoble metal salts. An almost dry slurry of carbon and metal salts was reduced using H₂ gas at temperatures of 600−850 °C, where the metals being treated determined the particular temperature. To achieve surface segregation of the noble metals, the thermal treatment was applied for 1−2 h. The following salts were used: AuCl₃, NiCl₂, K₂PtCl₄, CoCl₂, and PdCl₂, all obtained from Alfa Aesar. The molar ratio for the Au/Ni couple was 1:10, while for Pd:Co and Pt:Co it varied from 1:2 to 1:10. The elemental composition of nanoparticles was estimated based on the evidence of a complete reduction of the metal salts with which the high surface area carbon was impregnated. Rinsing the nanoparticles with water did not reveal the presence of any cation in solution.

Electrochemical (voltammetry and a UPD of Cu) and XRD measurements were used to verify the formation of stable core-shell structures. The peaks of the particle size distribution, found by TEM, are at 15 and 12 nm for Au/Ni and, Pd/Co and Pt/Co, respectively.

The method of platinum monolayer deposition by replacing a UPD Cu monolayer and the preparation of thin-film rotating disk electrodes were described in references.[7,8] Figure 1 displays a model description, i.e., an idealized picture, of the synthesis of core−shell nanoparticles and the deposition of Pt monolayer

* To whom correspondence should be addressed. E-mail: adzic@bnl.gov. Tel: +1−631-344-4522; Fax: +1−631-344-5815.
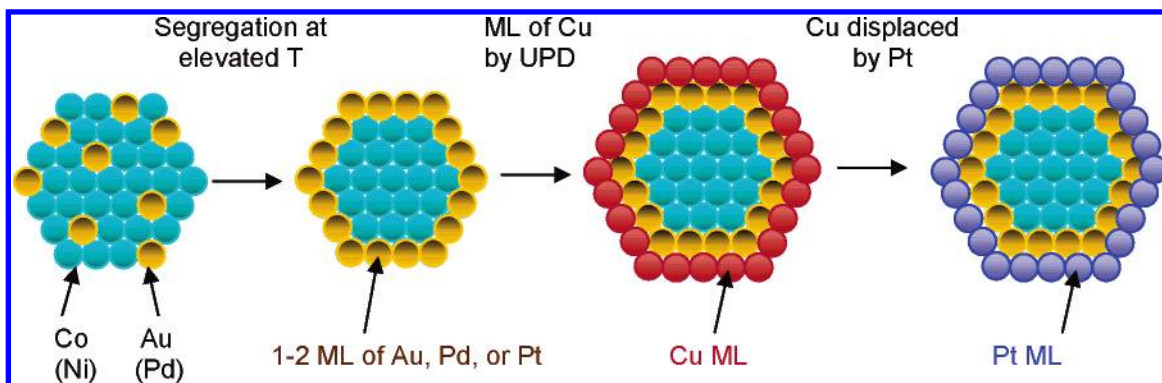† On leave from University of São Paulo, Brazil.

Figure 1. Model for the synthesis of Pt monolayer catalysts on nonnoble metal−noble metal core−shell nanoparticles.

on them. The content of noble metal used in forming a thin-layer electrode when deposited on a glassy carbon rotating disk electrode was the following: Pd in PdCo$_5$ 5.4 μg/cm^2, Au in AuNi$_{10}$ 4 μg/cm^2, and Pt in PtCo$_5$ 5 μg/cm^2. Solutions were prepared with Optima* sulfuric acid and perchloric acid obtained from Fisher, and MilliQ UV-plus water (Millipore). An Ag/AgCl/KCl (3 M) leak-free electrode was used as a reference, but all potentials, E, are quoted with respect to the reversible hydrogen electrode (RHE).

Results and Discussion

Synthesis and Characterization of Core−Shell Nanoparticles. The noble metal shell in the core−shell nanoparticle has two roles. First, it protects the nonnoble core from contacting the acid electrolyte; i.e., it precludes its dissolution. Second, the shell should improve the catalytic properties of a Pt monolayer by affecting its electronic properties and/or by inducing strain in a Pt monolayer that increases its activity. A strong surface segregation of a noble metal component is the key feature of these systems. For the host-solute systems investigated, viz., Ni−Au, Co−Pd, and Co−Pt, it was shown that a strong surface segregation of Au, Pd, and Pt in those alloys can be expected based on density functional theory (DFT) calculations,[10] and some experimental results.[11] The surface segregation of Au, Pd, and Pt and their protecting the Ni or Co core from dissolution was verified by linear sweep voltammetry, UPD of Cu, and X-ray diffraction technique.

The voltammetry curves (shown in Supporting Information) for the thin film electrodes of Au−Ni, Pd−Co, and Pt−Co nanoparticles revealed no anodic currents that can be ascribed to the oxidation/dissolution of Ni or Co, demonstrating that the cores are covered by the noble metal shell, and thus are inaccessible to the electrolyte solution. Some dissolution of Co or Ni probably takes place during the electrode preparation. The charges associated with this UPD of Cu on the Au−Ni, Pd−Co, and Pt−Co nanoparticles are 1.96, 2.26, 2.45 mC/cm^2, respectively, in good agreement with the real surface area that can be estimated from the particle sizes.[7,12] The UPD of Cu is ipso facto evidence that the surface mainly consists of a noble metal; it is not apparent on Co or Ni surfaces. The segregation and surface alloying of Au and Ni has been described in ref 13. The UPD of Cu on Pt, Pd, Au shells is quite well defined (Figure 1 in the Supporting Information), similar to the UPD on the nanoparticles of these metals. This synthetic method is applicable to a number of metal substrates, provided they do not form oxides in the UPD potential region for the metal used.

Figure 2 shows X-ray diffraction intensity profiles obtained for the Au/Ni$_{10}$ and pure Au (reference) particles. The strongest peak in the Au/Ni curve near 26.2 degrees corresponds to the
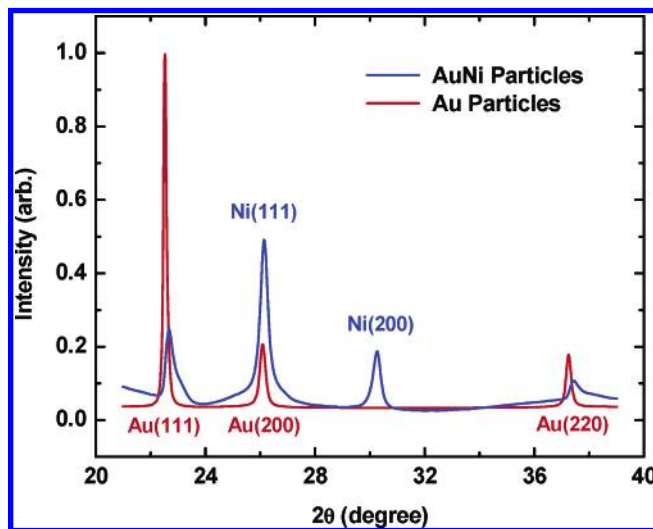

Figure 2. X-ray diffraction intensity profiles obtained with $\lambda = 0.922$Å at the beam line X7B at the National Synchrotron Light Source for the AuNi$_{10}$ and pure Au (reference) particles.

Ni(111) reflection at 26.2 and the Au(200) reflections at 26.1. In contrast to the symmetric peak at 30.33 corresponding to the Ni(200) reflection, the Au(111) and Au(220) peaks in the AuNi curve are nonsymmetrical and shifted to higher angles compared to those for the pure Au curve. This feature indicates that the Au is on top of the Ni particle, with a lattice contraction due to the lattice mismatch with the underlying Ni lattice (13% smaller than that of Au). The estimated thickness is about two monolayers. This result is in accord with the conclusions derived from the voltammetry data, and the UPD of copper on AuNi.

Oxygen Reduction Kinetics. Figures 3a−3c compare the polarization curves of the ORR on the electrocatalysts consisting of Pt monolayers on Au/Ni/C, Pd/Co/C, and Pt/Co/C substrates with that of the commercial Pt/C, all obtained using a thin film rotating disk electrode. All of the Pt monolayer electrocatalysts are more active than the Pt/C electrocatalyst. The differences in the half-wave potentials are 29, 25, and 45 mV for Pt/Au/Ni, Pt/Pd/Co, and Pt/Pt/Co, respectively. Comparing the activity of the electrocatalysts with different particle size is not a straightforward procedure because of their different real surface areas, but this does not affect our main conclusion. Figure 4 compares the activity of these electrocatalysts using the Pt mass activity and the total noble-metal mass activity (Pt plus the other noble metal), expressed as the current at 0.85 and 0.80 V. The enhancement in mass activity above that of the commercial Pt/C electrocatalyst ranges from about 2.5 to about 20 times, and 2.5 to about 4 times for Pt and the total noble metals, respectively.
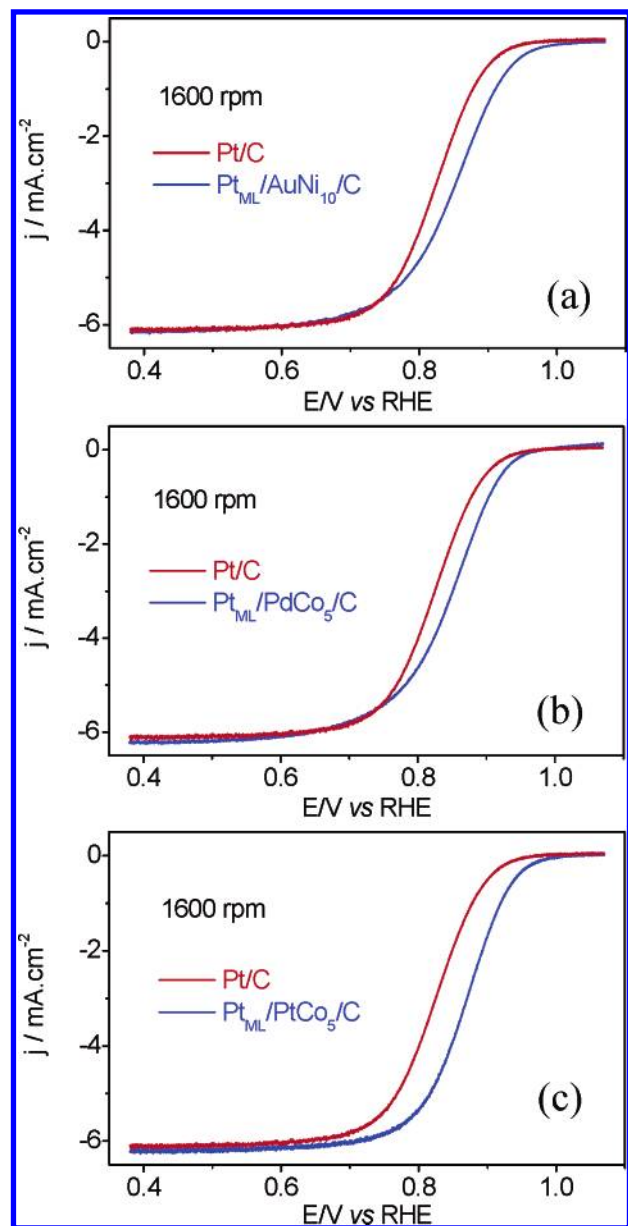
Letters

J. Phys. Chem. B, Vol. 109, No. 48, 2005 **22703**

Figure 3. Polarization curves for the ORR reduction on Pt monolayer electrocatalysts on carbon-supported $AuNi_{10}$, $PdCo_5$, and $PtCo_5$ core–shell nanoparticles in 0.1 M $HClO_4$. Sweep rate 10mV/s; room temperature.

Figure 4. (a) Pt mass activity of different electrocatalysts. (b) Total noble metal mass activity of different electrocatalysts.

In many ultrahigh vacuum studies,[14] the formation of a surface metal–metal bond significantly changed the electronic properties of metal overlayers, and pronounced differences were observed in the reactivity of some transition metal monolayers on various substrates.[14] According to Nørskov and co-workers,[15] the characteristics of the surface metal d-bands, particularly the weighted center of the d-band (ϵ_d), play a decisive role in determining surface reactivity. Previous DFT studies showed that compressive strain tends to downshift ϵ_d in energy, causing adsorbates to bind less strongly, whereas tensile strain has the opposite effect.[16] The position of the ϵ_d for the Pt monolayers also depends both on the strain (geometric effects) and on the electronic interaction between the Pt monolayer and its substrate (ligand effect).[17] Some interpretations of the monolayers' properties involve shifts of core levels due to a charge transfer between the monolayer and the substrate,[18] or changes in the density of states near the Fermi level.[19] An increased 5d vacancy of Pt, resulting from its interaction with a substrate metal, is believed to increase the interaction of O_2 and Pt, thereby
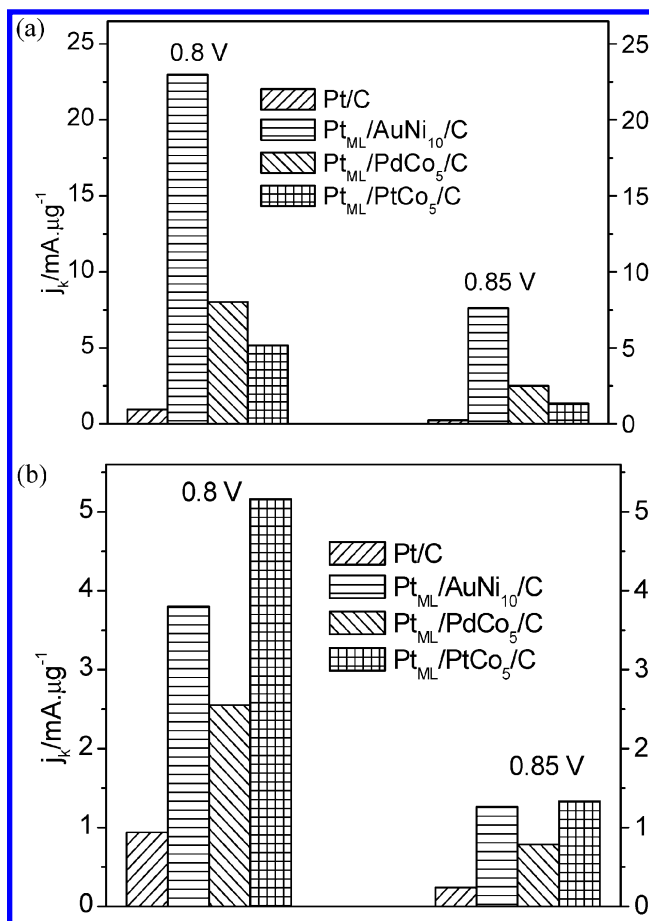
enhancing the catalytic activity of a Pt "skin" (several layers) on a PtNi or PtFe alloy.[6]

Earlier we demonstrated a nearly linear correlation between the binding energy of atomic oxygen on Pt monolayers on six single-crystal substrates and the corresponding ϵ_d.[8] The electrocatalytic activity of Pt monolayers on these surfaces shows a volcano-type dependence on the d-band center of the Pt monolayer structures, as determined by DFT calculations. The Pt monolayer supported on Pd(111) was the most active surface, at the top of the volcano curve. The superior catalytic activity of $Pt_{ML}/Pd(111)$ and the higher activity of Pt/Pd/C than that of Pt/C also was partly associated with a reduced PtOH coverage.[7]

The very high activities of Pt monolayers on Au/Ni, Pd/Co, and Pt/Co substrates for the ORR that surpass the catalytic activity of Pt/C appear to be a consequence of a mismatch in the lattice constants between the monolayers and these substrates, the changes in the d-band properties of the Pt monolayer itself caused by its interaction with them, and the decreased PtOH coverage. We assume that some level of pseudomorphism exists between the Pt monolayer and the nanoparticle surfaces. A possible mismatch between the lattice constants for a Pt monolayer on Pd/Co and Pt/Co, therefore, would be small, caused mostly by the contraction of Pt and Pd on the Co substrate. Consequently, it may generate only a very small compressive strain in a Pt monolayer, and, probably, a comparably small decrease in its reactivity due to such compression. However, activity for the ORR can increase as a result of a decline in PtOH adsorption. This is in agreement with the recent[20] analysis of water activation and a shift of PtOH formation to positive potentials for PtCo and PtFe alloys compared with Pt. The DFT calculations show a slight rise in
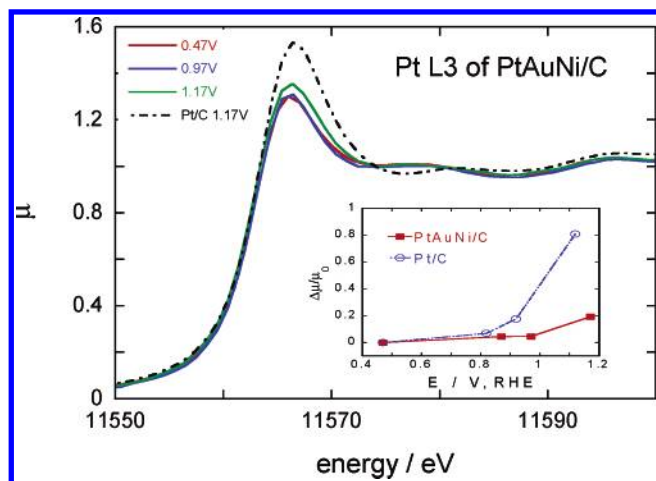
Figure 5. XANES spectra obtained with the Pt/Au/Ni/C electrocatalyst at 0.47 and 1.17 V and with Pt//C at 1.17 V in 1 M HClO$_4$, demonstrating a shift in Pt oxidation in Pt/Au/Ni/C. Inset: Relative change of the peak intensity ($\mu_E - \mu_{0.47}$)/$\mu_{0.47}$ for Pt in Pt/Au/Ni/C and in Pt/C as a function of potential obtained from the spectra.

activity for a pseudomorphic monolayer of Pt on a Pd(111) surface compared with one on Pt(111).[8] Therefore, an increase in activity can be expected for these surfaces.

For a Pt monolayer on AuNi particles, the monolayer is expected to be expanded, given the large difference between the Au and Pt lattices (4%). Accordingly, the band's center should be shifted upward and the binding energy of O$_2$ and the intermediates of its reduction should increase. This effect depends on the degree of pseudomorphism between the Pt monolayer and the Au/Ni substrate. The enhanced ORR kinetics observed for this surface indicates that the bonding apparently is not too strong, as is the case of a Pt monolayer on Au(111).[12] For the latter surface, a small inhibition in comparison with the reaction on Pt(111) is observed. This difference is probably due to the lesser expansion of Pt on AuNi than on Au(111), because of some contraction of the Au monolayer (bilayer) on the Ni core, which is observed in XRD data (Figure 2). In addition, the data obtained with in situ XANES show that the oxidation of a Pt monolayer is suppressed, occurring only at high potentials (1.17 V). This finding is verified by the size of the absorption peak for Pt in Pt/C, caused by the depletion of the d-band during the formation of PtOH, which is considerably larger than that for Pt/Au/Ni/C (Figure 5). The inset in Figure 5 shows the normalized change of absorption coefficient for the two surfaces. A decrease of PtOH formation can be due to an electronic (ligand) effect of the Au/Ni surface, while the decreased PtOH coverage can account for the greater activity of the Pt/Au/Ni electrocatalyst.

The enhanced activity of a Pt monolayer on a Pt/Co$_5$/C support compared with that of Pt/C might signify a fine-tuning of its electronic properties induced by the interaction with PtCo$_5$/C. Further work is required to elucidate this interesting phenomenon and its implications.

In conclusion, we demonstrated the synthesis of a new class of electrocatalysts consisting of a Pt monolayer deposited on nonnoble metal noble metal core−shell nanoparticles. We showed that it is possible to devise ORR electrocatalysts containing only a fractional amount of Pt and a very small amount of another noble metal whose activity can surpass that of the state-of-the-art carbon-supported Pt electrocatalysts. Consequently, the cost of fuel cells could be lowered considerably. Further work on these systems will address the question of their long-term stability.

Supporting Information Available: Supporting Information provides additional evidence for formation of the core−shell nanoparticles of AuNi$_{10}$, PdCo$_5$, and PtCo$_5$. The lack of Ni or Co dissolution, and the UPD of Cu observed in voltammetry curves, indicates that Au, Pd, or Pt forms shells around Ni or Co cores. This material is available free of charge via the Internet at http://pubs.acs.org.

References and Notes

(1) Tarasevich, M. R.; Sadkowski, A.; Yeager, E. Oxygen electrochemistry. In *Comprehensive Treatise of Electrochemistry*; Conway, B. E., Bockris, J. O., Yeager, E., Khan, S. U. M., White, R. E., Eds.; Plenum Press: New York, 1983; Vol. 7; p 301.

(2) Adzic, R. R. Recent advances in the kinetics of oxygen reduction. In *Electrocatalysis*; Lipkowski, J., Ross, P. N., Eds.; Wiley-VCH: New York, 1998; p 197.

(3) Gottesfeld, S.; Zawodzinski, T. A. In *Advances in Electrochemical Science and Engineering*; Alkire, R. C., Kolb, D. M., Eds.; Wiley-VCH: Weinham, 1997; Vol. 5; p 195.

(4) Brankovic, S. R.; Wang, J. X.; Adzic, R. R. *J. Serb. Chem. Soc.* **2001**, *66*, 887.

(5) Wang, J. X.; Markovic, N. M.; Adzic, R. R. *J. Phys. Chem. B* **2004**, *108*, 4127.

(6) Markovic, N. M.; Schmidt, T. J.; Stamenkovic, V.; Ross, P. N. *Fuel Cells* **2001**, *1*, 105.

(7) Zhang, J.; Mo, Y.; Vukmirovic, M. B.; Klie, R.; Sasaki, K.; Adzic, R. R. *J. Phys. Chem. B* **2004**, *108*, 10955.

(8) Zhang, J.; Vukmirovic, M. B.; Xu, Y.; Mavrikakis, M.; Adzic, R. R. *Angew. Chem., Int. Ed* **2005**, *44*, 2132.

(9) Brankovic, S. R.; Wang, J. X.; Adzic, R. R. *Surf. Sci.* **2001**, *477*, L173.

(10) Christoffersen, E.; Liu, P.; Ruban, A.; Skiver, H. L.; Norskov, J. K. *J. Catal.* **2001**, *199*, 123.

(11) Bardi, U. *Rep. Prog. Phys.* **1994**, *57*, 939.

(12) Zhang, J.; Vukmirovic, M. B.; Sasaki, K.; Uribe, F.; Adzic, R. R. *J. Serb. Chem. Soc.* **2005**, *70*, 513.

(13) Molenbroek, A. M.; Nørskov, J. K.; Clausen, B. S. *J. Phys. Chem. B* **2001**, *105*, 5450.

(14) Rodriguez, J. A. *Surf. Sci. Rep.* **1996**, *24*, 223.

(15) Hammer, B.; Nørskov, J. K. *Adv. Catal.* **2000**, *45*, 71.

(16) Xu, Y.; Ruban, A. V.; Mavrikakis, M. *J. Am. Chem. Soc.* **2004**, *126*, 4714.

(17) Kitchin, J. R.; Nørskov, J. K.; Barteau, M. A.; Chen, J. G. *J. Chem. Phys.* **2004**, *120*, 10240.

(18) Mukerjee, S.; Soriaga, M.; McBreen, J. *J. Phys. Chem.* **1995**, *99*, 4577.

(19) Ruckman, M. W.; Strongin, M. *Acc. Chem. Res.* **1994**, *27*, 250.

(20) Murthi, V. S.; Urian, R. C.; Mukerjee, S. *J. Phys. Chem. B* **2004**, *108*, 11011.